

## Internal gettering in epi-silicon prepared under different conditions

This article has been downloaded from IOPscience. Please scroll down to see the full text article.

2002 J. Phys.: Condens. Matter 14 13127

(<http://iopscience.iop.org/0953-8984/14/48/359>)

View [the table of contents for this issue](#), or go to the [journal homepage](#) for more

Download details:

IP Address: 171.66.16.97

The article was downloaded on 18/05/2010 at 19:16

Please note that [terms and conditions apply](#).

# Internal gettering in epi-silicon prepared under different conditions

C Frigeri<sup>1</sup>, G Borionetti<sup>2</sup> and P Godio<sup>2</sup>

<sup>1</sup> CNR-IMEM Institute, Parco Area delle Scienze 37/A, Fontanini, 43010, Parma, Italy

<sup>2</sup> MEMC Electronic Materials SpA, Viale Gherzi 31, 28100 Novara, Italy

E-mail: Frigeri@maspec.bo.cnr.it

Received 27 September 2002

Published 22 November 2002

Online at [stacks.iop.org/JPhysCM/14/13127](http://stacks.iop.org/JPhysCM/14/13127)

## Abstract

The efficiency of internal gettering in epi-silicon was studied in samples prepared under different conditions as compared to external gettering and p<sup>+</sup> gettering. The parameters changed were substrate resistivity, oxygen content and presence/absence of poly-Si on the back-side. The efficiency of internal gettering was assessed by measurement of the electron-beam-induced-current contrast versus temperature and applying existing models for interpreting the results. Internal gettering is effective also in p<sup>+</sup> substrates with poly-Si on the back-side when the density of oxygen precipitates is high and their size small. Internal gettering is not effective for low density of oxygen precipitates when either p<sup>+</sup> substrates or poly-Si or both are used.

## 1. Introduction

Deep levels in the band gap associated with metallic impurities present in semiconductors strongly affect the lifetime of the minority carriers. As regards silicon, the 3d transition metallic atoms (e.g. Mo, Fe, Cu, Ni) are inevitably introduced into the Si wafers during the wafer processing following the crystal growth step. The high diffusivity of those metals in Si further contributes to making their presence harmful. The concentration level of metal impurities that can be tolerated is mainly determined by the dimensions of the devices and is now set at  $1 \times 10^{10} \text{ cm}^{-3}$  or below. To reduce the contamination level to such a value in the active device region, gettering procedures are used whereby the metallic atoms are removed from some regions of the wafers to other pre-determined ones where their presence is not harmful (Myers *et al* 2000).

Various gettering techniques are used, such as internal gettering, high-boron-concentration-activated gettering, external gettering in the modes of (Gay and Martinuzzi 1997, Myers *et al* 2000): (a) back-side poly-Si gettering, (b) Al back-side gettering (Al–Si alloying),

(c) phosphorus diffusion gettering and (d) gettering at nanocavities introduced by helium or hydrogen implantation (Williams *et al* 1999). According to the physical mechanism operating, the above procedures may also be classified as relaxation or segregation or injection-induced gettering (Myers *et al* 2000, Schröter *et al* 1992).

Internal or intrinsic gettering involves oxygen precipitates, often associated with dislocations, as sinks for the metallic impurities (Myers *et al* 2000, Hieslmair *et al* 1998, Laczik *et al* 1996, Gilles *et al* 1990). The oxygen precipitates are intentionally created in the wafer, e.g., by an appropriate three-step (Hi–Lo–Hi) annealing process. By back-side poly-Si external gettering, the impurities are gettering by the grain boundaries of a polycrystalline Si layer deposited on the back of the wafer. High-boron-concentration-activated gettering applied to Fe is due to the electronic interactions between Fe interstitials and the dopant B ions controlled by the temperature-dependent Fermi-level position (Benton *et al* 1996, Stolk *et al* 1996). It can be applied to p/p<sup>+</sup> epitaxial structures with the epilayer having a p concentration smaller than the boron concentration of the p<sup>+</sup> substrate, that becomes thus a sink for the metal atoms. The use of p/p<sup>+</sup> epitaxial structures in Si technology has the advantage of the active region (built in the epilayer) being unaffected by the crystal-originated particles (COPs), because any possible COP remains localized at the substrate surface, and of reducing the latch-up of the devices (McHugo *et al* 1998).

Here we present a study of the efficiency of internal and poly-Si external gettering as well as substrate p<sup>+</sup> doping gettering in p/p<sup>-</sup> and p/p<sup>+</sup> epi-silicon, based on Cz material prepared in different ways. Gettering efficiency assessment was carried out through the observation of the non-radiative recombination properties of oxygen precipitates by analysis of the slope of the curves of the electron-beam-induced-current (EBIC) contrast versus temperature.

## 2. Experimental details

Two types of epi-structure have been investigated, i.e., p/p<sup>-</sup> and p/p<sup>+</sup>. For each type of substrate two different oxygen contents were used, namely 11.5–12.5 ppma ('low oxygen') and 14–15 ppma ('high oxygen'). For some samples poly-Si was deposited on the back of the substrate by chemical vapour deposition (CVD) at 680 °C. The B-doped p<sup>-</sup> and p<sup>+</sup> Cz substrates had resistivities of 10–20 Ω cm and 5–10 mΩ cm, respectively, a diameter of 200 mm and were (100) oriented. Single-wafer epi-reactors have been used to deposit the epitaxial layers. No HCl baking was applied during epi-deposition. The epilayers were 2 and 4 μm thick for the p/p<sup>-</sup> and p/p<sup>+</sup> cases, respectively, with the resistivity of 10 Ω cm. The epi-structures have been subjected to a 64 MDRAM device thermal simulation in a horizontal furnace with inert or oxidizing ambient for a total thermal cycle of 23 h. Temperatures ranged from 750 to 1100 °C depending on the actual intended purpose in device fabrication, i.e. film deposition, gate oxidation, field oxidation, dopant drive-in.

Schottky diodes were prepared by sputtering Al on the epi-surface. They were used to carry out EBIC measurements in a scanning electron microscope as a function of temperature  $T$  from 73 to 300 K by using an Oxford cryostage. The beam energy used was in the range 30–40 keV with beam currents between 0.5 and 5 pA. The contrast (%) at the non-radiative recombination centres detected by means of EBIC was evaluated as  $C = (I_0 - I_d)/I_0$  where  $I_0$  is the EBIC signal collected far from the recombination centre and  $I_d$  is the EBIC signal at the defect.

Transmission electron microscopy (TEM) in the bright-field mode was also used to determine the structure of the oxygen precipitates. The cross-section TEM specimens were prepared by mechanical thinning followed by Ar-ion beam bombardment.

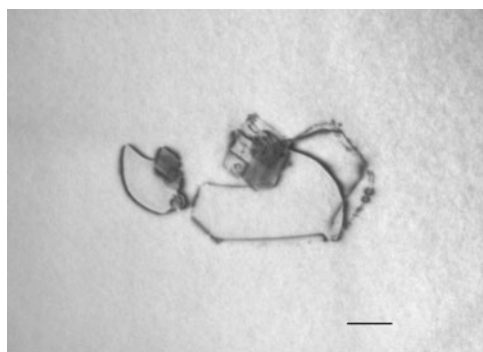


**Figure 1.** A TEM image of an oxygen precipitate/dislocation complex in a sample  $p/p^+$ , high oxygen content, with poly-Si on the back-side. The bar is 200 nm.

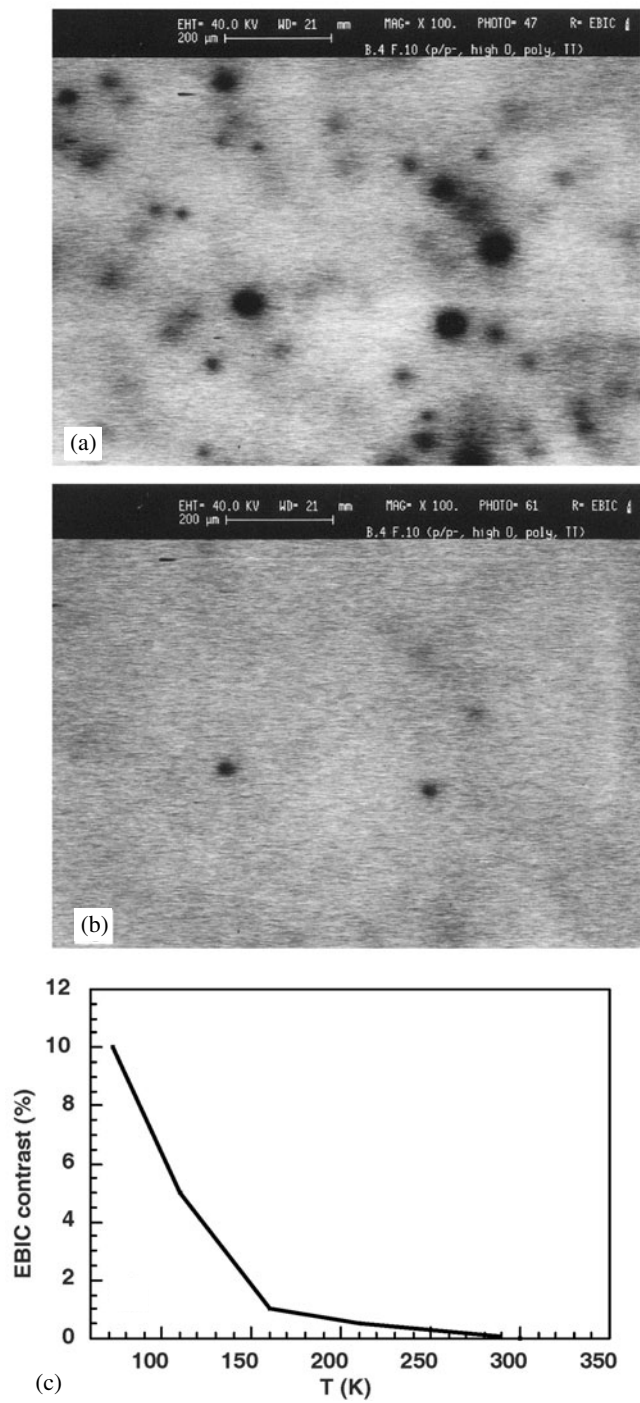
### 3. Results and discussion

Figure 1 is a TEM image of the crystallographic defects present in the substrates of the samples investigated. The TEM image was taken from the  $p/p^+$  sample with high oxygen content. The defects are oxygen precipitates and dislocation loops that punch out from them. The precipitates are of the octahedron type, consistently with the annealing temperature used (Sueoka *et al* 1994, Fujimori 1997). The density of oxygen precipitates was measured by decorative etching. For the  $p/p^-$  case it was  $10^6$  and  $10^7$   $\text{cm}^{-3}$  for low and high oxygen contents, respectively. For the  $p/p^+$  samples it was  $5 \times 10^8$  and  $10^{10}$   $\text{cm}^{-3}$  for low and high oxygen contents, respectively.

#### 3.1. $p/p^-$ , at high oxygen content: internal versus external gettering

A comparison is first made of the influence of back-side poly-Si on the internal gettering efficiency. Figures 2(a)–(b) are EBIC images of the  $p/p^-$  epi-structure with back-side poly-Si and high oxygen content, taken at 73 and 160 K, respectively. The EBIC contrast at the oxygen precipitates and associated dislocation(s) at 160 K is lower than at 73 K. It vanishes completely at 300 K (image not shown). The EBIC contrast versus temperature is plotted in figure 2(c). The contrast curve has a negative slope. When no poly-Si was present, all the other parameters ( $p/p^-$ , high oxygen content) being constant, EBIC contrast was also visible at 300 K where it was greater than at lower temperatures. A typical EBIC contrast versus  $T$  curve for the case of no back-side poly-Si is shown in figure 3.

The interpretation of the EBIC contrast curves is based on the model of Kittler and Seifert (1994, 1996) including the latest contribution of Kveder *et al* (2001). The EBIC detectability of the electrical activity at all temperatures including RT, with a positive slope of the contrast versus  $T$  curve, as seen for the no-poly-Si sample (figure 3), indicates that in this sample the oxygen precipitate/dislocation complexes are contaminated with impurities having some associated deep level in the Si band gap (Kittler and Seifert 1994, 1996, Kveder *et al* 2001). Similar conclusions can be arrived at by applying the model of Wilshaw *et al* (1989, 1995). In our case, such impurity is expected to be Fe since Fe has been found by DLTS to be the main metallic impurity present in samples prepared in the same way as the samples used here, with a density of about  $5 \times 10^{11}$   $\text{cm}^{-3}$  (Borionetti and Godio 2000). The model given by Kveder *et al* (2001) suggests that the energy level of the contaminating impurity has to be at an energy  $\geq 0.35$  eV from the valence band. Interstitial Fe with the energy level of  $E_v + 0.39$  eV, with  $E_v$  the valence band edge, meets this condition.



**Figure 2.** Sample  $p/p^-$ , high oxygen content, with poly-Si on the back-side. EBIC images at (a) 73 K and (b) 160 K. (c) Curve summarizing the behaviour of the EBIC contrast (%) versus temperature  $T$  between 73 and 300 K.

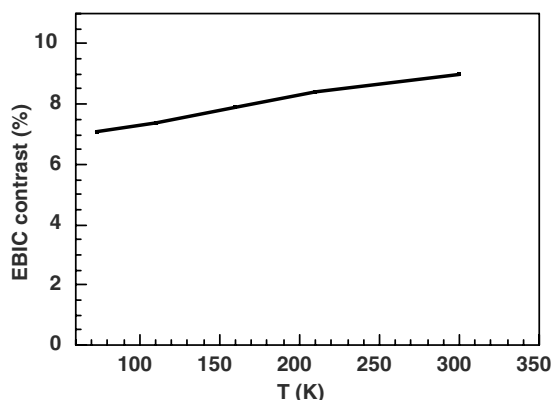


**Figure 3.** Sample  $p/p^-$ , high oxygen content, with no poly-Si on the back. Curve summarizing the behaviour of the EBIC contrast (%) versus temperature  $T$  in the range 73–300 K.

On the other hand, the negative slope of the EBIC contrast versus  $T$  curve, with vanishing EBIC contrast as  $T$  increases to RT, for the sample with poly-Si (figure 2(c)) indicates that the observed electrical activity at low temperatures is due to minority carrier recombination at the shallow levels intrinsic to the crystal defects (Kveder *et al* 2001). Very probably the shallow levels are those of the dislocations punched out from the oxygen precipitates. This type of EBIC contrast is characteristic of ‘clean’ dislocations (Kittler and Seifert 1994, 1996, Kveder *et al* 2001). With poly-Si on the back, therefore, the metallic impurities do not contaminate the oxygen precipitate/dislocation complexes, unlike in the case when poly-Si is absent. External gettering seems thus to prevail over internal gettering for  $p^-$  substrates when both are present.

### 3.2. $p/p^+$ versus $p/p^-$ , high oxygen content, poly-Si: comparison of internal, external and $p^+$ gettering

Next, the influence of the substrate resistivity is examined for the case where poly-Si is also present on the back-side. The  $p/p^+$  and  $p/p^-$  samples with high oxygen content are first considered. Figure 4(a) shows an EBIC image at 300 K for a sample  $p/p^+$  with high oxygen content and poly-Si. EBIC contrast at the oxygen precipitate/dislocation complexes is detectable and remains so even on decreasing the temperature, though with a smaller value, as shown in the plot of figure 4(b). The non-radiative recombination area at the defects is smaller in this sample due to the smaller size of the oxygen precipitates in  $p^+$  silicon.

As above, following the model of Kittler and Seifert (1994, 1996) and Kveder *et al* (2001), the latter results suggest that in the  $p/p^+$  samples with high oxygen content, Fe contamination of the oxygen precipitate/dislocation complexes takes place, so that internal gettering of Fe seems to be effective despite the presence of poly-Si on the back-side and the high doping level of the  $p^+$  substrate which can both cause Fe gettering.

The effect of  $p^+$  doping on the gettering of Fe has been discussed by some authors for as-grown  $p^+$  substrates or B-implanted silicon, mainly of the FZ type, for which it seems to be the prevailing gettering mechanism for heavy p doping due to the enhanced solubility of Fe (Aoki *et al* 1995, Benton *et al* 1996, Stolk *et al* 1996, McHugo *et al* 1998).

The action of Fe gettering in a  $p/p^+$  structure takes place by two concomitant mechanisms (Benton *et al* 1996, Stolk *et al* 1996). The first one is the formation of  $Fe_i^+ - B^-$  pairs, where  $Fe_i^+$  is the positive charged state of the interstitial Fe,  $Fe_i$ . In p-type Si,  $Fe_i$  becomes positively

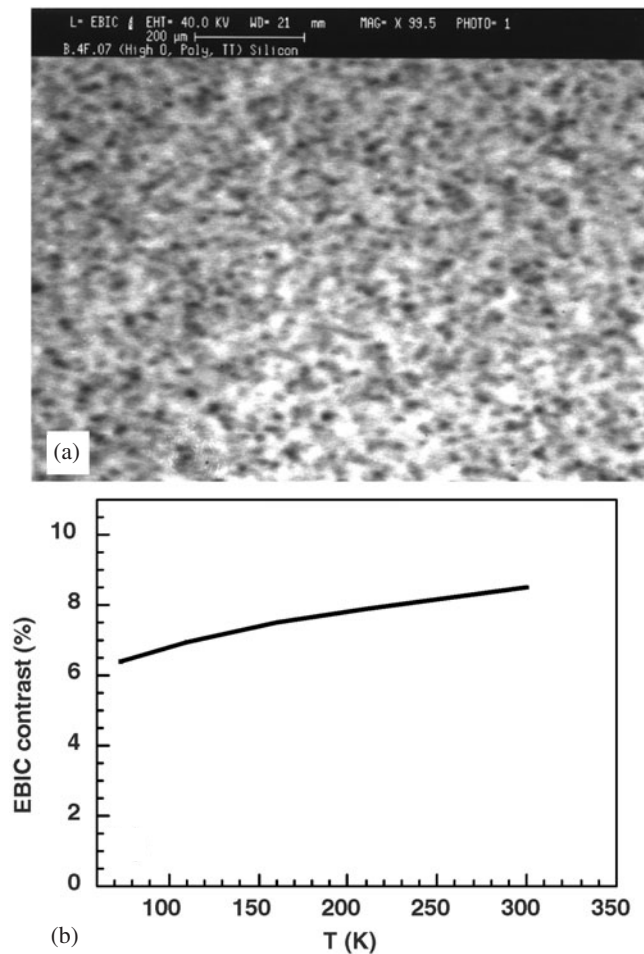


**Figure 4.** Sample p/p<sup>+</sup>, high oxygen content, with poly-Si on the back. (a) An EBIC image at 300 K. (b) Curve summarizing the behaviour of the EBIC contrast (%) versus temperature  $T$  between 73 and 300 K.

charged when the Fermi level is below the deep-level state of  $\text{Fe}_i$  which is at  $E_v + 0.39$  eV. The Fermi-level-controlled fraction of  $\text{Fe}_i^+/\text{Fe}_i^0$ , where  $\text{Fe}_i^0$  is the Fe in the neutral state, is a function of p doping (B content) and temperature  $T$  and increases for increasing p ([B]) and decreasing  $T$  (Benton *et al* 1996). A Coulomb attraction arises between  $\text{Fe}_i^+$  and  $\text{B}^-$  with the formation of  $\text{Fe}_i^+-\text{B}^-$  pairs (Benton *et al* 1996). The second mechanism is the redistribution of Fe between the p and p<sup>+</sup> regions. The higher number of negative ions in the p<sup>+</sup> region exerts a Coulomb attraction on the  $\text{Fe}_i^+$  ions that then migrate from the p region to the p<sup>+</sup> substrate (Benton *et al* 1996). The ratio of  $\text{Fe}_i^+$  in the highly B-doped region to that in the less doped region increases exponentially with decreasing  $T$  (Benton *et al* 1996). Gettering of Fe in the p<sup>+</sup> regions is due to the simultaneous action of both Fermi-level-induced Fe redistribution and Fermi-level-controlled Fe–B pairing. The theory of the Fermi-level dependence of Fe gettering by p<sup>+</sup> regions predicts that such gettering is possible only for  $T < 600$  °C, since above this temperature the electronic effects discussed above are too weak. It becomes extremely effective at temperatures below 400 °C (Benton *et al* 1996).

Our results show that internal gettering is effective in  $p/p^+$  structures based on Cz substrates when the level of oxygen is 'high' (14–15 ppma in our case). This can be explained by considering that precipitation of Fe at the oxygen precipitates on cooling from the annealing temperature can occur at temperatures higher than 400 °C. Hieslmair *et al* (1998) reported that efficient internal gettering at the precipitates can take place above 520 °C. On the other hand, at temperatures lower than 400 °C, i.e. when  $p^+$  gettering is also operative, it is likely that some of the Fe atoms are trapped at the oxygen precipitates instead of forming Fe–B pairs. The high density of oxygen precipitates in the  $p^+$  substrate may favour internal gettering by increasing the number of trapping sinks, as reported by other authors (Hieslmair *et al* 1998, McHugo *et al* 1995). Such competition between the two different sinks (precipitates and Fe–B pairs) does not exist in FZ Si where oxygen precipitates are not expected and  $p^+$  gettering may be the only operative gettering mechanism. It should be noted that internal gettering can also benefit from the increase of the solubility of Fe due to the high B concentration. According to the work of McHugo *et al* (1998), for  $p = 1 \times 10^{19} \text{ cm}^{-3}$  (resistivity of 10 m $\Omega$  cm) the solubility for Fe is  $5 \times 10^{11} \text{ cm}^{-3}$  for temperatures between 650 and 700 °C, so that Fe precipitation can start at such temperatures, i.e. earlier than the expected onset of  $p^+$  gettering.

It should be noted that in the case now discussed ( $p/p^+$ , high oxygen content, poly-Si on the back), internal gettering is operative even in the presence of the back-side poly-Si that was shown above to prevail over internal gettering for  $p^-$  substrates. Internal gettering can be competitive with external gettering in this case due to the higher density of oxygen precipitates in  $p^+$  substrates with respect to the  $p^-$  ones, which makes them much closer to each other than in the case of smaller density ( $p^-$  substrates). This property can increase the trapping probability of Fe atoms at the precipitates before they reach the back-side poly-Si.

The EBIC results for the  $p/p^-$ , high-oxygen-content, poly-Si case are those already given in figure 2. In this case internal gettering does not work. Very probably, trapping of Fe at the oxygen precipitates is negligible due to their low density. Since the substrate resistivity is high, gettering should only be due to the back-side poly-Si.

### 3.3. $p/p^+$ versus $p/p^-$ , low oxygen content, poly-Si: comparison of internal, external and $p^+$ gettering

For low oxygen content and poly-Si on the back, both  $p/p^+$  and  $p/p^-$  samples exhibit similar EBIC behaviour, i.e. EBIC contrast curves with negative slope similar to that given in figure 2(c) with no detectable EBIC contrast at high temperatures. This indicates negligible internal gettering and dominance of external gettering for the  $p/p^-$  samples. For the  $p/p^+$  case our results do not allow us to say whether  $p^+$  gettering or external gettering prevails. It is possible that external gettering at poly-Si dominates, because diffusion of Fe to the back-side is expected to occur at temperatures higher than 400 °C, which is the temperature at which  $p^+$  gettering starts to be really effective (Benton *et al* 1996), and therefore at an earlier time than the  $p^+$  gettering.

## 4. Summary

In  $p/p^+$  epi-structures based on Cz substrates with high density of oxygen precipitates, a condition obtained with high oxygen content using our thermal treatment,  $p^+$  gettering seems to be less important than internal and external gettering, since it is expected to take place effectively only at temperatures lower than 400 °C (Benton *et al* 1996), whereas the other two mechanisms occur at higher temperatures, i.e., at an earlier time on cooling. Experimental evidence of internal gettering was obtained through EBIC experiments even in the presence of



back-side poly-Si, and hence of possible external gettering, and is believed to be likely due to the high density of small oxygen precipitates with associated dislocations. At present it is not possible to say to what extent the different gettering mechanisms contribute to trapping of the Fe atoms.

For  $p/p^+$  samples with low densities of oxygen precipitates, a condition obtained with low oxygen contents, internal gettering was not detected. In such a case our techniques do not allow us to establish to what extent external gettering and  $p^+$  gettering are operative. Qualitative speculations based on the temperature dependence of the two mechanisms would suggest that external gettering prevails.

For  $p/p^-$  samples, internal gettering has not been seen to be effective when back-side poly-Si was applied, so only external gettering should be active as  $p^+$  gettering is not expected to work. Internal gettering worked instead when no poly-Si was applied.

### Acknowledgment

This work was supported by PN Microelettronica (5%).

### References

- Aoki M, Itakura T and Sasaki N 1995 *Appl. Phys. Lett.* **66** 2709
- Benton J L, Stolk P A, Eaglesham D J, Jacobson D C, Cheng J-Y, Ha N T, Haynes T E and Myers S M 1996 *J. Appl. Phys.* **80** 3275
- Borionetti G and Godio P 2000 unpublished results
- Fujimori H 1997 *J. Electrochem. Soc.* **144** 3180
- Gay N and Martinuzzi S 1997 *Solid State Phenom.* **57–58** 115
- Gilles D, Weber E R and Hahn S 1990 *Phys. Rev. Lett.* **64** 196
- Hieslmair H, Istratov A A, Heiser T and Weber E R 1998 *Appl. Phys. Lett.* **72** 1460
- Kittler M and Seifert W 1994 *Mater. Sci. Eng. B* **24** 78
- Kittler M and Seifert W 1996 *Mater. Sci. Eng. B* **42** 8
- Kveder V, Kittler M and Schröter W 2001 *Phys. Rev. B* **63** 115208
- Laczik Z, Bouwhuis L, Booker G R and Falster R 1996 *Solid State Phenom.* **47–48** 177
- McHugo S A, McDonald R J, Smith A R, Hurley D L and Weber E R 1998 *Appl. Phys. Lett.* **73** 1424
- McHugo S A, Weber E R, Mizuro M and Kirscht F G 1995 *Appl. Phys. Lett.* **66** 2840
- Myers S M, Seibt M and Schröter W 2000 *J. Appl. Phys.* **88** 3795
- Schröter W, Seibt M and Gilles D 1992 *Mater. Sci. Technol.* **4** 540
- Stolk P A, Benton J L, Eaglesham D J, Jacobson D C, Cheng J-Y, Poate J M, Myers S M and Haynes T E 1996 *Appl. Phys. Lett.* **68** 51
- Sueoka K, Ikeda N and Yamamoto T 1994 *Appl. Phys. Lett.* **65** 1686
- Williams J S, Conway M J, Wong-Leung J, Deenapanray P N K, Petravic M, Brown R A, Eaglesham D and Jacobson D C 1999 *Appl. Phys. Lett.* **75** 2424
- Wilshaw P R and Fell T S 1995 *J. Electrochem. Soc.* **142** 4298
- Wilshaw P R, Fell T S and Booker G R 1989 *Point and Extended Defects in Semiconductors Part 2*, ed G Benedek, A Cavallini and W Schröter (New York: Plenum) p 243